Journal of Archaeological Science: Reports 37 (2021) 102984

Contents lists available at ScienceDirect

Journal of Archaeological Science: Reports

journal homepage: www.elsevier.com/locate/jasrep

A four-stage approach to re-associating fragmented and commingled human remains

Rebecca L. Bourgeois [a,*], Vladimir I. Bazaliiskii [b], Hugh McKenzie [c], Terence N. Clark [d], Angela R. Lieverse [d]

[a] Department of Anthropology, University of Alberta, 13–15 Tory Building, University of Alberta, Edmonton, AB T6G 2H4, Canada
[b] Baikal Region Research Centre, Irkutsk State University, 1 Karl Marx Street, Irkutsk, Irkutsk Oblast 664003, Russia
[c] Department of Anthropology, Economics and Political Science, MacEwan University, 7–367D, City Centre Campus, 10700–104 Avenue, Edmonton, AB T5H 0S5, Canada
[d] Department of Archaeology and Anthropology, University of Saskatchewan, 55 Campus Drive, Saskatoon, SK S7N 5B1, Canada

ARTICLE INFO

Keywords:
Bioarchaeology
Poor preservation
GIS
Osteometric analysis
Osteology
Life history
Middle Holocene

ABSTRACT

Bioarchaeological and forensic anthropological methods are limited in their ability to re-associate human skeletal remains that have been both fragmented and commingled. Although many methods for individualizing commingled remains exist, they are rendered ineffective when the level of fragmentation is high. In these contexts, human remains are often approached similarly to faunal assemblages, regarded as sets of fragmented elements rather than as groups of fragments representing an individual. This paper introduces a new, four-stage approach to identifying discrete individuals from unintentionally fragmented and commingled human remains and salvaging information from highly disturbed cemetery contexts. These stages include documentation, grouping, analysis, and evaluation, each incorporating multiple methods so as to be applicable to a wide variety of assemblages or data availability. Through this process, quantitative analyses are used to evaluate qualitative groupings. This method is applicable to skeletal collections of varying levels of preservation. To demonstrate its application, we apply this methodology to an Early Neolithic (7560–6660 HPD cal. BP) hunter-gatherer cemetery, Moty-Novaia Shamanka (MNS), located in the Cis-Baikal region of Siberia, Russia. MNS was destroyed in the 1990s for urban development and flood management, leaving the ancient skeletal remains severely fragmented and commingled. Our results identified five discrete individual groupings from 1245 human bone fragments, and eight further groupings of related fragments. Through a process of elimination, it was determined that these groupings represented at least seven distinct people. The methodological approach of this study challenges our perception of the informative value of fragmented and commingled human remains and provides an example of how future studies could approach individualization in situations where most context has been lost.

1. Introduction

Contemporary human activity, such as urban and industrial development, is among the main driving forces that both destroy and displace interred human remains, risking the loss of archaeological and other cultural heritage (Foster and Lovekamp, 2015; Maples and East, 2013; Rainville, 2009; UNESCO, 2018). Unfortunately, it is common for unmarked cemeteries and burials to be discovered through development, their remains being commingled and fragmented in the process (Killoran et al., 2016). The literature addressing the problem of how to sort commingled human remains is extensive (e.g., Adams and Byrd, 2006; Adams and Konigsberg, 2008; Byrd, 2008; Byrd and Adams, 2003; Finlayson et al., 2017; Herrmann and Devlin, 2008; Karell et al., 2016; LeGarde, 2019; Mundorff et al., 2014; Osterholtz et al., 2014b; Perrone et al., 2014; Rodrìguez et al., 2016; Ubelaker, 2002; Zejdlik, 2014), but each methodological approach to this problem is limited by fragmentation. This paper presents a four-stage approach for identifying discrete individuals from fragmented and commingled human remains. To do so, it considers the poorly preserved and highly fragmented remains from the Early Neolithic (EN, 7560–6660 HPD cal. BP; Bronk Ramsey et al.,

* Corresponding author.
E-mail address: rbourgeo@ualberta.ca (R.L. Bourgeois).

https://doi.org/10.1016/j.jasrep.2021.102984
Received 31 March 2021; Accepted 5 April 2021
Available online 13 May 2021

2021; Weber et al., 2021) hunter-gatherer Kitoi cemetery Moty-Novaia Shamanka (MNS) in the Cis-Baikal region of Siberia (Russian Federation). As a new and unique Kitoi site, MNS has substantial research potential, especially with the identification of discrete individuals. Existing methods used to salvage information from highly disturbed contexts—such as those applied in zooarchaeology, forensic anthropology, and bioarchaeology—were modified and further developed using the MNS collection, creating a template for other researchers to apply in similar situations. As this four-stage approach was developed in a context where fragmentation was high, it is applicable to collections of varying levels of preservation. The methodology is particularly relevant for long-term usage commingled assemblages (Osterholtz et al., 2014a), such as destroyed cemetery sites. Like all methods focused on the re-association of commingled and fragmented remains, some aspects of this methodology, such as general element groupings and spatial analysis, will be more successful when applied to small skeletal assemblages. However, this approach is broadly applicable to a wide variety of bioarchaeological and forensic contexts.

2. Materials

In the 1990s, a low-lying hill was bulldozed during the development of the village of Novaia ("New") Shamanka, along the Irkut River in Siberia's Cis-Baikal region, in order to mitigate flooding (Bazaliiskii et al., 2016). Originally located on this hill was the EN cemetery of MNS. The cemetery was destroyed, and the human remains left fragmented and commingled within a garden plot for about twenty years until the property owner contacted archaeologists at Irkutsk State University. In 2014 and 2015, MNS was partially excavated by VI Bazaliiskii in three excavations (Fig. 1). Excavation I was conducted in a series of three trenches. Trench A (green) was excavated in 2014 along the eastern fence line of the property and was expanded in 2015 into trenches B (blue) and C (red). Excavation II was centered around an area of ochre staining that was underneath a house at the time of the bulldozing, crushing the remains rather than pushing them across the site. Excavation III was dug at the northwest corner of the property to clear the area for a future building. In addition to this, test units (TU 2–4) were also excavated at the northwest corner of the property surrounding Excavation III. Neither Excavation III nor the tests units yielded any human remains (Bazaliiskii et al., 2016). The only other osteological analysis of the MNS human skeletal collection was a population size estimate of 19 adult individuals in Excavation I by Denis Pezhemsky (Lomonosov University, Moscow; Bazaliiskii et al., 2016). These methods, however, remain unreported and are not included in this study. As a whole, the MNS collection is comprised of 1245 fragments of generally poor condition, ranging from small, unidentifiable fragments to a few nearly complete bones. The high level of fragmentation from the bulldozing was accompanied by red ochre staining as typical for the Kitoi mortuary tradition, biodegradation from the natural environment, bleaching and weathering of those fragments exposed to the elements, and etching from plant roots, all affecting the surface features and quality of each fragment. For more detailed description of the MNS collection, please refer to Bourgeois (2020).

3. Methods

A four-stage approach (Fig. 2) was developed to collect both qualitative and quantitative data with which to re-associate fragments into discrete individuals. This process created hypothetical groupings based on qualitative data (visual grouping) that were then tested

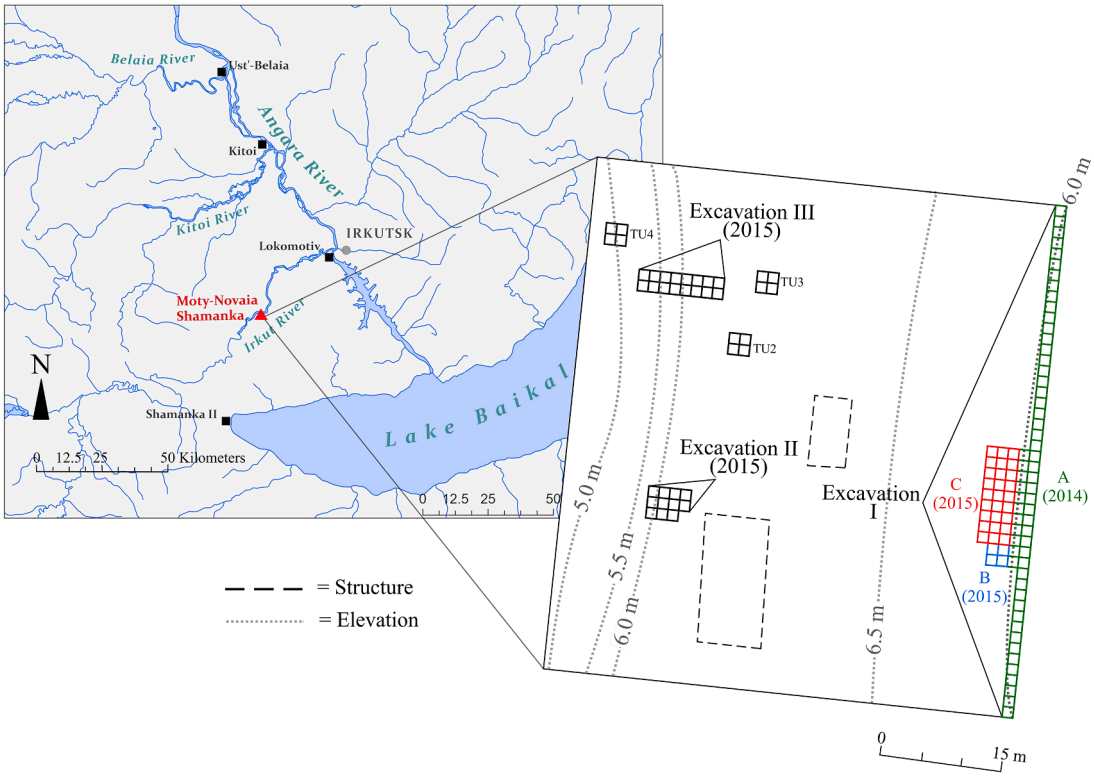

Fig. 1. Location of MNS and archaeological site plan of the 2014, 2015 Excavations I–III. Major Kitoi sites mentioned in the Early Neolithic section noted by black squares. The focal site of this paper, Moty-Novaia Shamanka, is noted by a red triangle. Sites obtained from Weber et al., 2010 and Bazaliiskii et al., 2016. Data was freely obtained from DIVA-GIS (http://www.diva-gis.org/) and NATURAL EARTH (https://www.naturalearthdata.com/). Regional map created in ArcGIS Pro by William T.D. Wadsworth. Excavation plan drawn and modified from those provided by lead archaeologist of the MNS excavations (co-author VI Bazaliiskii).

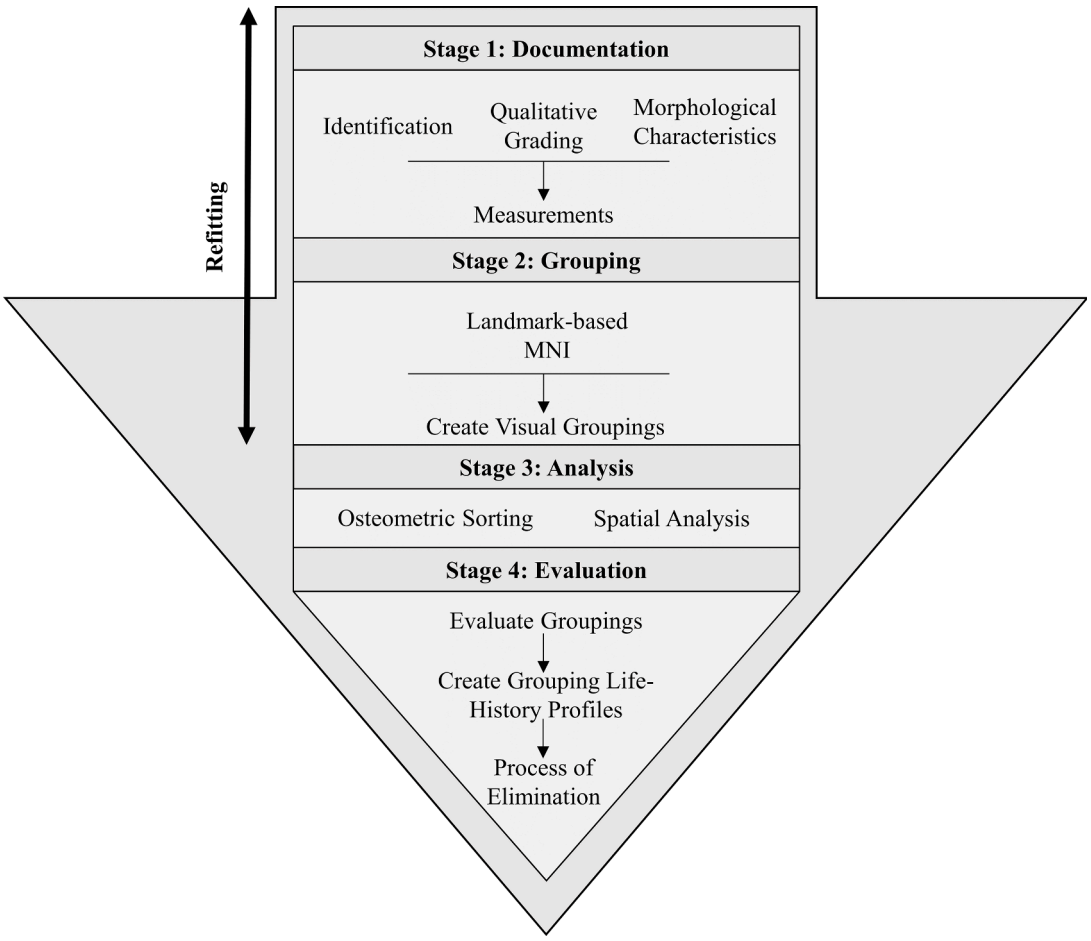

Fig. 2. The four-stage approach taken to identify discrete individuals from the MNS collection.

quantitatively to either support or reject their association.

3.1. Stage 1: Documentation

Stage 1 included the bulk of the data collection. Herein each of the 1245 fragments in the MNS collection was identified and recorded using the Zonation Method (Dobney and Reilly, 1988; Knüsel and Outram, 2004; Outram, 1998, 2001; Outram et al., 2005). Owing to the varying levels of preservation within the collection, which often limited the ability to identify fragments, an evaluation scale for fragment identifiability was created (Table 1). This scale ranged from unidentifiable (Degree 0) to nearly complete bones that were able to be identified to specific element and side (Degree 5). Next, each fragment was graded qualitatively based on stage of weathering (Behrensmeyer, 1978 as modified and described by Buikstra and Ubelaker, 1994) and level of ochre staining (Table 2). In the case of MNS, weathering and ochre staining are a reflection of both the original burial and the post-disturbance environments. It is likely that bones from the same individual would have experienced broadly similar depositional environments for the vast majority of their postmortem histories (i.e., 6600+ years), but the recent disturbance could account for differences in weathering and ochre staining patterns. Therefore, these criteria were only used as descriptive measures of the bone surface that supported a grouping after multiple other criteria indicated that fragments were from the same individual.

Morphological characteristics were also noted for each fragment. These included entheseal morphology, non-metric traits (according to Buikstra and Ubelaker, 1994; Finnegan, 1978; Hauser and De Stefano, 1989; Saunders, 1978), pathological and degenerative changes (Buikstra and Ubelaker, 1994; Gestsdóttir, 2014; Lieverse et al., 2007, 2016; Mays

Table 1
Fragment identifiability.

Degree	Description
0	Fragment is very small and unidentifiable.
1	Fragment is small but identifiable to class (such as a costal, limb long bone, vertebral, or cranial vault fragment).
2	Fragment is identifiable to element with a few exceptions (metacarpals, metatarsals, and phalanges are not identifiable to specific element), but not identifiable to side.
3	Fragment is identifiable to element and side, but less than 50% of the bone is represented; it can be used for MNI.
4	Fragment is identifiable to element and side, with 50–75% of the bone represented; postmortem damage is localized to a specific end or area.
5	Fragment is identifiable to element and side, representing 76–100% of the element with little to no postmortem damage.

The line between degrees 3 and 4 signifies the two different goals of this grading system. Degrees zero through three describe the main usefulness of the fragment to this study and the individualization process, whereas degrees four and five provide further details in the context of this study and inform future scholars on the completeness of the fragment.

Table 2
Evaluation scale for ochre staining.

Level	Description of Ochre Staining
0	No ochre staining
1	Very light ochre staining
2	Light to moderate ochre staining
3	Dark ochre staining

and Holst, 2006; Ortner, 2003; Purchase, 2016), stages of development, dental wear (Smith, 1984; Scott, 1979; as referenced in Buikstra and Ubelaker, 1994), calculus deposition (Brothwell, 1981; as presented in Buikstra and Ubelaker, 1994), sexually dimorphic traits, and indicators of age at death (Acsádi and Nemeskéri, 1970; Bass, 1995; Buikstra and Ubelaker, 1994). A SuniRay handheld x-ray was used to determine if tooth absence was congenital, pathological, or developmental. After each fragment was described, standard measurements were taken (Buikstra and Ubelaker, 1994; Moore-Jansen et al., 1994; White, 1977; Suwa, 1990; White et al., 2012), as were those used for stature reconstruction from fragmented human remains (De Mendonça, 2000; Steele, 1970; Steele and McKern, 1969; Wright and Vásquez, 2003). As per standard practice, measurements were recorded as an average of three, taken using digital calipers. To maximize the comparative potential between fragments, landmark-based measurements were developed to accommodate the poor preservation of the MNS collections (all measurements used are summarized in Table 3). Although fragment refitting occurred throughout this stage (see below), measurements avoided areas that were reconstructed, as this process may affect their accuracy, and thus that of subsequent osteometric sorting (Stage 3).

3.2. Stage 2: Grouping

All fragments of identifiability Degree 3 and higher (Table 1) were then sorted by element and used in the calculation of a landmark-based MNI (Mack et al., 2016) for comparison to the population size estimate of 19 individuals by Pezhemsky (Bazaliiskii et al., 2016). This MNI included one individual from Excavation II, which was from a separate excavation and contained at least one of each skeletal element even if they were not able to be specifically identified. Visual groupings were made independent of the landmark-based MNI and based on qualitative characteristics recorded in the Documentation stage (such as size and morphology). These served as hypotheses that were tested during the analysis stage (Stage 3) and included both general groupings and bilateral element pairings. Throughout the first two stages, where possible, fragments were refit to form conjoins of two or more fragments (as in Osterholtz, 2012a, 2012b, 2014, 2018; Osterholtz et al., 2014b).

3.3. Stage 3: Analysis

During this stage, the provisional groupings made during Stage 2 were tested using osteometric sorting and spatial analysis. Bilateral elements were tested using both osteometric sorting and spatial analysis, whereas other grouped elements were tested only with spatial analysis. Osteometric sorting followed the methods outlined by Thomas and colleagues (2013) based on studies of the level of bilateral asymmetry within a large sample of human skeletons from a variety of populations (spanning various time periods and geographic regions). Only those fragments that were visually paired were tested osteometrically to evaluate their provisional grouping. This comparison used the M statistic ($M = |L–R| / [(L + R)/2]$), where M was the test statistic quantifying the relative difference between paired measurements, L represented the measurement on the left bone, and R represented the same measurement taken on the right bone (Thomas et al., 2013). The M statistic generated from MNS-hypothesized pairs was compared to the 90th and 95th percentiles, as well as the maximum value of aggregate male and female values in the reference sample tables (which they calculated for their sample population using a linear interpolation algorithm in Microsoft Excel; Thomas et al., 2013) to test the null hypothesis (H_0) that the two paired fragments were from the same individual. In cases where poor preservation prohibited taking the same measurement as documented in the reference literature (Thomas et al., 2013), the MNS measurement (see Table 3) was compared to the most similar measurement from the reference sample. In cases where articular surfaces are preserved, unlike MNS, osteometric methods for re-associating articularting remains (such as Byrd and LeGarde, 2014)

Table 3
List of measurements that were taken on various elements in the MNS collection.

Element	Description of Measurements (recorded in mm)
Mandible	Breadth of the mandibular body[1]
	Height of the mandibular body[1]
	Maximum and minimum ramus breadths[1]
	Maximum ramus height[1]
	Buccolingual and mesiodistal crown diameters of all teeth[3]
Clavicle	Maximum diameter at the conoid tubercle
	Superior-inferior diameter at the conoid tubercle
	Maximum diameter at the medial aspect of the trapezoid line
	Maximum diameter at the lateral aspect of the trapezoid line
	Superior-inferior breadth at the medial aspect of the trapezoid line
	Superior-inferior breadth at the lateral aspect of the trapezoid line
Scapula	Maximum mediolateral breadth of the glenoid fossa
	Maximum superoinferior breadth of the glenoid fossa
	Maximum superoinferior breadth of the acromion
	Maximum mediolateral breadth of the acromion
	Minimum diameter of the most lateral portion of the scapular spine joining the acromion to the body of the wing medial to the glenoid fossa
	Mediolateral breadth of the coracoid
Humerus	Epicondylar breadth[1]
	Vertical diameter of head[1]
	Maximum diameter at midshaft[1]
	Minimum diameter at midshaft[1]
	Midshaft circumference
	Anteroposterior diameter at the most inferior point of the deltoid tuberosity where it meets the crest for the greater tubercle
	Mediolateral diameter at the most inferior point of the deltoid tuberosity where it meets the crest for the greater tubercle
	Circumference at the most inferior point of the deltoid tuberosity where it meets the crest for the greater tubercleMaximum diameter at the most inferior point of the deltoid tuberosity where it meets the crest for the greater tubercle
	Minimum diameter at the most inferior point of the deltoid tuberosity where it meets the crest for the greater tubercle
	Anteroposterior diameter at the most inferior point of the crest for the lesser tubercle where it meets the medial crest
	Mediolateral diameter at the most inferior point of the crest for the lesser tubercle where it meets the medial crest
	Circumference at the most inferior point of the crest for the lesser tubercle where it meets the medial crest
	Maximum diameter at the most inferior point of the crest for the lesser tubercle where it meets the medial crest
	Minimum diameter at the most inferior point of the crest for the lesser tubercle where it meets the medial crest
	Maximum length[1]
	Mediolateral breadth of the olecranon fossa
	Superoinferior breadth of the olecranon fossa
	Anteroposterior breadth of the shaft at the point where the lateral side of the deltoid tuberosity begins to angle distomedially
	Diameters of the deltoid tuberosity at the point where the lateral side begins to angle medially (anteroposterior, mediolateral, maximum, minimum)
	Circumference of the shaft at the point where the lateral side of the deltoid tuberosity begins to angle distomedially
Radius	Midshaft diameters (anteroposterior and mediolateral midshaft)[1]
	Maximum diameter immediately superior to radial tuberosity
	Mediolateral breadth of the radial tuberosity
	Anteroposterior sub-radial tuberosity diameter immediately distal to the radial tuberosity
	Mediolateral sub-radial tuberosity diameter immediately distal to the radial tuberosity
	Maximum sub-radial tuberosity diameter immediately distal to the radial tuberosity
	Minimum sub-radial tuberosity diameter immediately distal to the radial tuberosity
	Sub-radial tuberosity circumference immediately distal to the radial tuberosity
Ulna	Anteroposterior diameter[1]
	Mediolateral diameter[1]
	Anteroposterior diameter at the most inferior point where the pronator ridge meets with the diaphysis immediately proximal to the distal end
	Mediolateral diameter at the most inferior point where the pronator ridge meets with the diaphysis immediately proximal to the distal end
	Maximum diameter at the most inferior point where the pronator ridge meets with the diaphysis immediately proximal to the distal end

(*continued on next page*)

Table 3 (*continued*)

Element	Description of Measurements (recorded in mm)
	Minimum diameter at the most inferior point where the pronator ridge meets with the diaphysis immediately proximal to the distal end
	Circumference at the most inferior point where the pronator ridge meets with the diaphysis immediately proximal to the distal end
	Mediolateral diameter at the coronoid process
	Anteroposterior diameter at the coronoid process
	Distance from the medial side of radial notch to lateral edge of the trochlear notch
	Anteroposterior diameter of the olecranon
	Mediolateral diameter of the olecranon
Femur	Anteroposterior subtrochanteric diameter[1]
	Mediolateral subtrochanteric diameter[1]
	Anteroposterior midshaft diameter[1]
	Mediolateral midshaft diameter[1]
	Midshaft circumference[1]
	Anteroposterior diameter at the point where gluteal and spiral lines join the linea aspera
	Mediolateral diameter at the point where gluteal and spiral lines join the linea aspera
	Maximum diameter at the point where gluteal and spiral lines join the linea aspera
	Minimum diameter at the point where gluteal and spiral lines join the linea aspera
	Circumference at the point where gluteal and spiral lines join the linea aspera
	Bicondylar breadth[1]
	Mediolateral breadth of the lesser trochanter
	Superoinferior breadth of the lesser trochanter
Tibia	Mediolateral diameter at the nutrient foramen[1]
	Maximum diameter at the nutrient foramen[1]
	Minimum diameter at the nutrient foramen[1]
	Circumference at the nutrient foramen[1]
	Anteroposterior diameter at the point where anterior crest crosses over to the medial border of the shaft proximal to the medial malleolus[2]Mediolateral diameter at the point where anterior crest crosses over to the medial border of the shaft proximal to the medial malleolus[2]
	Maximum diameter at the point where anterior crest crosses over to the medial border of the shaft proximal to the medial malleolus[2]
	Minimum diameter at the point where anterior crest crosses over to the medial border of the shaft proximal to the medial malleolus[2]
	Circumference at the point where anterior crest crosses over to the medial border of the shaft proximal to the medial malleolus[2]
	Mediolateral intercondylar breadth
	Maximum anteroposterior diameter of the diaphysis not including the medial malleolus
Fibula	Anteroposterior diameter at the point where the interosseous crest meets the surface for interosseous ligaments
	Mediolateral diameter at the point where the interosseous crest meets the surface for interosseous ligaments
	Maximum diameter at the point where the interosseous crest meets the surface for interosseous ligaments
	Minimum diameter at the point where the interosseous crest meets the surface for interosseous ligaments
	Circumference at the point where the interosseous crest meets the surface for interosseous ligaments
	Anteroposterior diameter at the nutrient foramen
	Mediolateral diameter at the nutrient foramen
	Maximum diameter at the nutrient foramen
	Minimum diameter at the nutrient foramen
	Circumference at the nutrient foramen
	Anteroposterior diameter at the superior point of the attachment site for the interosseous ligament
	Mediolateral diameter at the superior point of the attachment site for the interosseous ligament
	Maximum diameter at the superior point of the attachment site for the interosseous ligament
	Minimum diameter at the superior point of the attachment site for the interosseous ligament
	Circumference at the superior point of the triangular subcutaneous are
Calcaneus	Middle breadth[1]
	Maximum distance between the medial and posterior talar facets
	Distance between the most posterior point of the posterior talar facet and the most anterior edge of the calcaneal tuberosity
Talus	Maximum breadth (diameter from the most medial point of the medial malleolar surface to the most lateral point of the lateral process)
	Mediolateral diameter of the trochlear surface (taken at approximately the midpoint)
	Distance from the most medial point of the lateral process to the most lateral point of the lateral process
	Maximum breadth of the sulcus tali (space between the posterior and medial subtalar facets)
	Maximum diameter of the posterior subtalar facet
	Maximum length (from the most anterior point on the head to the most posterior point)

1, Measurements taken according to Moore-Jansen et al., 1994, as reproduced by Buikstra and Ubelaker 1994; 2, Measurements taken according to Steele and McKern (1969) and Steele (1970); 3, Measurement taken according to White (1977) and Suwa (1990, pp. 40–43) as cited in White and colleagues (2012). Those without notation were developed during this study.

would be useful to include at this stage.

For the spatial analysis, ArcGIS 10.4 was used to make renderings of the original site plans of Excavation I. Excavation II was omitted from spatial analysis because it was a separate area of the site with a different disturbance history and the position of each fragment was not recorded at the time of excavation. These renderings included a point for the location of each fragment (or group of clustered fragments) *in situ*, which was then linked to the catalogue that was compiled in the documentation stage. The maximum distance between two fragments within a conjoin were taken to represent the furthest distance that two known pieces of the same bone travelled within the site. X and Y coordinates for each fragment or fragment cluster (n = 1072) were generated using GIS and inputted into PAST (Paleontological Statistics Software Package for Education and Data Analysis version 2.17) to generate a distance matrix of pair-wise comparisons from point to point using Euclidean geometry. This created 572,987 distances, in meters, of which the mean and standard deviation were calculated using Excel and were used to describe the general proximity of fragments to one another. The mean and standard deviation of the distance between all points within Excavation I formed the indices of proximity, when combined with the maximum known distance travelled by a conjoin. These indices were used to test the proximity of grouped fragments.

Two associated fragments were defined as having *high proximity* if the distance between them was less than the maximum distance between two conjoins (2.09 m) plus an arbitrary buffer of 2 m. The arbitrary value of the buffer was a reasonable approximation that accounts for both the mean height of the human skeleton (1.58 m; Auerbach and Ruff, 2010) and the average grave length at the nearby Kitoi cemeteries of Shamanka II and Lokomotiv (~2 m), both excavated by co-author VI Bazaliiskii. This reference for the average height of a human skeleton is consistent with other studies done in the area such as that by Temple and colleagues (2014), who referred to their stature estimation formula for use on EN adults from the Cis-Baikal region. Thus, any fragments within 4.09 m of one another were considered to have *high proximity*. Two fragments were classified as having *moderate proximity* if they were within the cut-off for high proximity (4.10) and one standard deviation (derived from the site wide distance matrix) above the mean distance of all points within Excavation I (6.77 m). Anything beyond this distance (6.78+ m) was considered to have *low proximity*. As this method is enhanced by distance data from conjoined fragments, it is likely more precise in cases of small-scale commingling, as is typical of methodologies addressing commingled human remains. Nevertheless, this approach to spatial analysis is broadly applicable to a wide variety of bioarchaeological and forensic contexts, depending on field preparation, data availability, and commitment to the refitting process.

3.4. Stage 4: Evaluation

Herein each grouping of associated fragments was evaluated based

on their distinctiveness from other groupings. Based on the quantitative and qualitative data that supported a grouping of fragments, they were categorized as either an *Individual* or an *Association*. Those classified as an *Individual* possessed characteristics that set them apart from all other groupings, therefore being confidently distinct from other Individuals. Those classified as an *Association* consisted of multiple fragments that were able to be grouped together but were not distinct enough to rule out a relationship with other groupings; therefore, there could have been some overlap between different Associations or between Associations and Individuals. Associations are thus auxiliary groupings of related elements that supplement studies of life history. They also play into the following process of elimination that was employed to clarify the possibility of overlap between Individuals and Associations. Individual groupings were not compared to one another because they were already deemed to be discrete. The process of elimination considered distinguishing characteristics, any overlap between element representation, and proximity. It did not emphasize the qualitative evaluation criteria that described the depositional and post-depositional environment (such as ochre staining and weathering). Instead, it prioritized the consideration of each Individual and Association as a set of skeletal elements that were cross-referenced with all other groupings in order to identify those that could not possibly represent the same individual. More detailed information on this four-stage multi-method is presented in Bourgeois (2020). The possibility of overlap was classified as not possible (No) if there was a definitive reason why two groupings could not be from the same individual (such overlapping element representation or inconsistent stage of development); unlikely (UL) if they had differing morphological characteristics or low proximity, making it unlikely that these groupings were from the same individual, but a possible relationship could not be definitively eliminated; and possible (PSB) if the groupings had high proximity and there were no definitive measures (representation or stage of development) that opposed their grouping. In the latter case, although groupings were separated by our four-stage approach, it is still possible that they could represent the same individual. In all cases, proximity was measured as the distance between the closest fragments within each grouping.

4. Results and discussion

Here we report on the application of this method to the MNS site. 71.16% of the MNS collection was identifiable to element class (Degree 1), but only 41.04% was identifiable to a specific element (Degree 2 or higher). Of the 1245 total fragments, 202 (16.23%) were able to be refitted to form 74 conjoins. Stage 2 yielded an MNI of nine, based on femoral fragments. This calculation included the assumed presence of one of each element in Excavation II, which did not result in any duplication (because of the large distance between excavations). The MNI served as one objective estimate of population size, and a first step toward individualization. From these remains, five discrete Individuals were identified, represented by groups of multiple fragments (Fig. 3). A further eight Association groupings were identified (Fig. 4), but these were not conclusively distinct from all other groupings and so could not be classified as distinct Individuals. Through process of elimination (Table 4), we determined that these 13 groupings (five Individuals and eight Associations) represented at least seven people. This was evident when the extra sets of lower limbs (Associations A, B, and C) were compared to the Individual groupings made up of solely upper limbs (Individuals 1 and 2). Individual 2 was excluded due to the distinct gracile morphology (see below) of the remains that was not shared by the three lower limb Associations. As Individual 1 could only be associated with one set of lower limbs, there were at least two other people, in addition to the five Individuals, represented by these groupings. Our analysis demonstrated that none of the Individuals overlapped with any other Individual; therefore, we are confident that the groupings made in

Fig. 3. All discrete Individuals identified in this study. They are indicated according to their identification number.

Fig. 4. All Association groupings identified in this study. They are indicated according to their alphabetical identification.

this study represent at least seven people, five discrete (represented by Individuals) and at least two others that are identifiable through a process of elimination (represented by two of Associations A, B, or C). Association groupings are summarized in Table 5 and described in Bourgeois (2020), but they are not discussed here.

4.1. Individual 1

Individual 1 was represented by a partial cranium, mandible, right scapula, right humerus, and both clavicles. Qualitatively, this grouping was made on the basis of very pronounced entheses and characteristic bright-red ochre staining. The maxilla and mandible had congenitally absent left and right third molars and similar, moderate, wear patterns that fit together when articulated. Minor dental calculus (code 1 according to Brothwell, 1981) was present on most teeth, and the moderate level of tooth wear suggested a young adult age at death. Sex was indeterminate, since some observable traits (gonial angle) were robust, consistent with males, while others were ambiguous (mastoid process) or more consistent with females (nuchal crest, posterior zygomatic process; Acsádi and Nemeskéri, 1970; Bass, 1995; Buikstra and Ubelaker, 1994). This individual's generally robust cranial morphology is typical for Middle Holocene (ca. 8630–3470 HPD cal. BP; Bronk Ramsey et al., 2021; Weber et al., 2021) occupants of the Cis-Baikal, both male and female. As a result, sex assessment based on only a few cranial morphological indicators is generally ineffective for these populations. Pronounced humeral and clavicular entheses suggested well-developed deltoid, trapezius, latissimus dorsi, and pectoralis major muscles, consistent with watercraft use during life (e.g., Lieverse et al., 2009). This individual showed signs of moderate periodontitis in both jaws and antemortem breakage of the left mandibular central incisor. Fine-grained pitting on, and destruction of, the right external auditory meatus suggested chronic otitis externa (Mays and Holst, 2006; Purchase, 2016). Observable non-metric traits included a mylohyoid bridge on the mandible and a suprascapular notch and circumflex sulcus on the scapula (Buikstra and Ubelaker, 1994; Finnegan, 1978; Saunders, 1978; Winder, 1981). The furthest distance between two fragments was 2.20 m

Table 4
Potential relationships between Individual and Association groupings based on a process of elimination.

	1	2	3	4	5	A	B	C	D	E	F	G	H
1		No	No	No	No	PSB^{h}	PSB^{h}	PSB^{h}	No	PSB^{h}	PSB^{h}	No	No
2			No	No	No	UL^{m}	UL^{h}	UL^{h}	No	No	PSB^{m}	PSB^{m}	PSB^{m}
3				No	No	No	No	No	No	No	No	No	No
4					No	No	No	No	PSB^{h}	PSB^{h}	PSB^{h}	UL^{l}	PSB^{h}
5						No	No	No	No	No	No	No	No
A							No	No	PSB^{m}	PSB^{h}	PSB^{h}	UL^{l}	PSB^{h}
B								No	PSB^{h}	PSB^{h}	PSB^{h}	UL^{l}	PSB^{h}
C									PSB^{h}	PSB^{h}	PSB^{m}	UL^{l}	PSB^{m}
D										PSB^{m}	PSB^{m}	UL^{l}	PSB^{m}
E											PSB^{h}	UL^{l}	PSB^{h}
F												PSB^{m}	PSB^{h}
G													No
H													

No, no possible relationship based on the types of fragments present in the groupings; UL (unlikely), relationship cannot be entirely ruled out based on element representation, but it is less likely because of morphological characteristics or low proximity (measurements based on distance between closest fragments); PSB (possible), possible relationship between two groupings. ^{h}Fragments had high proximity; ^{m}Fragments had moderate proximity; ^{l}Fragments had low proximity.

(mean = 0.98 m; sd = 0.73), putting them in high proximity. When bilateral clavicular measurements were compared to Thomas and colleagues' (2013) midshaft diameters, the null hypothesis was not rejected in any case, further supporting their grouping.

4.2. Individual 2

Individual 2 included the right arm of an adult female. This grouping was initially based on the small size of the skeletal elements and their defined entheses. Both the radial head and the olecranon epiphysis were fused, indicating a minimum age of 14–15 years at death (Schaefer et al., 2009:199, 213). Morphological comparisons to juveniles (15–20 years) and small-bodied adults from the nearby Kitoi sites of Shamanka II and Lokomotiv, however, revealed that these were the remains of an adult (20+ years). All anatomical landmarks (e.g., interosseous borders) were well-defined, and entheses (e.g., supinator crest, ulnar tuberosity, deltoid tuberosity, and crest for the greater tubercle) were pronounced. The small body size suggested a likely female sex, particularly considering a study of sexual dimorphism in Kitoi populations that showed statistically significant differences in robusticity between males and females (Stock et al., 2010). The bones' small size was not evidence of bone atrophy because entheses were well developed and diaphyseal morphology was normal, rather than being diminished or altered as has been documented in cases of disuse atrophy (e.g., Lieverse et al., 2008). The maximum distance between two fragments was 0.72 m (mean = 0.49 m; sd = 0.32); therefore, these fragments were in high proximity.

4.3. Individual 3

Individual 3 represented the left leg of an adolescent of indeterminate sex. Each fragment showed distinct, bright-red ochre staining supporting their grouping. This Individual was an excellent example of how the process of refitting fragments greatly influenced interpretations and the grouping process. Comprised of 13 previously unidentifiable fragments conjoined into four bone segments, the refitting process allowed for the left femur, and its apophyseal cutback zone indicating

Table 5
Summary of association groupings.

Group	No. of fragments	Elements Represented	Sex	Age	Pathological lesions	NMTs	Osteometric sorting	Proximity
A	3	Right Tibia; Right Fibula; Left Fibula;	N/A	Adult	Diffuse periosteal bone formation,[1] some remodeled.[2]	N/A	N/A	High (max/ mean = 1.61 m)
B	5	Left Tibia; Right Tibia; Left Fibula; Right Fibula;	N/A	Adult	N/A	Squatting facets on both left and right distal tibiae	Supports grouping	High (max = 0.45 m, mean = 0.35 m, sd = 0.16)
C	2	Left Femur; Left Tibia	N/A	Adult	N/A	N/A	N/A	High (max/mean = 1.84 m)
D	3 (incl. 1 conjoin)	Left Humerus; Right Humerus	N/A	Adult	N/A	N/A	Supports grouping	High (max = 0.26 m, mean = 0.18, sd = 0.08)
E	2 (incl. 1 conjoin)	Left Radius; Left Ulna	N/A	Adult	N/A	N/A	N/A	High (max/mean= 0.98 m)
F	2	Atlas (C1 vertebra); Axis (C2 vertebra)	N/A	Adult	Degenerative changes on the dens (axis) and dens facet (atlas) consistent with vertebral osteoarthritis	N/A	N/A	High (max/ mean=0.37 m)
G	16 (incl. 2 conjoins)	Cranial vault	N/A	Adult	Ectocranial porosity on the posterior right parietal	Retained metopic suture	N/A	High (max = 0.33 m, mean = 0.21 m, sd = 0.10)
H	15 (incl. 2 conjoins)	Cranium	Possibly female[3]	Adult	Destruction and fine-grained pitting of the right external auditory meatus, suggesting chronic otitis externa	Right supraorbital notch, left zygomatico-facial foramen, left supraorbital foramen, left marginal tubercle[4]	N/A	High (max = 1.47 m, mean = 0.87 m, sd = 0.45)

[1] On the posteromedial border of the left fibula as well as on the anterior crest and posterior and anterior borders of the tibia.
[2] On the tibial diaphysis.
[3] Glabella (3), supraorbital margin (4), mastoid process (Acsádi and Nemeskéri, 1970), a posterior zygomatic process that did not extend posterior to the external auditory meatus (Bass, 1995).
[4] Buikstra and Ubelaker, 1994; Hauser and De Stefano, 1989; Oettlé et al., 2017.

stage of development, to be identified. The cutback zone provided an age at death estimate between 14 and 18 years based on comparison to a wide range of juvenile femora from Shamanka II and Lokomotiv. These comparisons focused on the morphology and robusticity of the bone and the presence of the porous cutback zone inferior to the lesser trochanter, which was a sign of the tapering of the diaphysis during development (Lewis, 2018: 4–5: Reddi, 1981). Owing to the lower levels of completeness, no non-metric traits were observable. The maximum distance between two fragments was 2.17 m (mean = 1.53 m; sd = 0.59), putting them in high proximity.

4.4. Individual 4

Individual 4 included the lower limb bones of an adult of indeterminate age and sex. These fragments were initially grouped based on their characteristic light yellow-orange ochre staining, complementary smooth entheses, and uniquely high level of weathering. The latter could reflect a similar depositional environment consistent with these remains having been from the same individual. Osteometric sorting of the paired tibiae showed that all measurements rejected the null hypothesis at both the 90th and 95th percentiles, as well as the maximum value for M within the reference sample (Thomas et al., 2013). The one exception, the maximum diameter at the nutrient foramen, only rejected the null hypothesis at the 95th percentile and the maximum value for M. Considering that the difference between the M value of the two MNS tibiae and the reference sample was 0.003 and that the bones show postmortem surface degradation, these values could still be considered as supporting the grouping of tibial fragments. Moreover, the exact position of the tibial nutrient foramen is variable within an individual, introducing error to measurements based on this landmark (Mead and Christensen, 2020; Vehit and Christensen, 2019). Due to the lower level of completeness, no non-metric traits were observable in this individual. The maximum distance of two fragments was 3.83 m (mean = 2.30 m; sd = 1.48), suggesting high proximity.

4.5. Individual 5

Individual 5 included all fragments from Excavation II, which were not labelled individually because the archaeologists excavating the site determined, *in situ*, that these were the remains of one individual that was not commingled with others. Analysis of the fragments from this excavation did not indicate any duplication of elements, supporting this claim. Individual 5 consisted of 255 total bone fragments making up 11 post-cranial conjoins. The poor level of preservation and identifiability prevented age and sex estimation and was most likely the cause of the variable levels of ochre staining and weathering observed. Of the 11 conjoins, two were identifiable as a right humerus and a right femur and two others as portions of an unsided metatarsal and femur. The zone representation of the unsided femur did not overlap with the identified right; therefore, it did not indicate more than one person in Excavation II. Other conjoins were not definitively identifiable but, based on shape and size, they could possibly be from a femur, humerus, and a fibula. Remaining fragments represented portions of the left and right scapulae, right ilium, right femur, an ulna, calcaneus, metatarsal, and probable parietal bone. Eleven phalangeal fragments, 191 long bone fragments, and 20 unidentified bone fragments were also recovered. Due to the low level of preservation, no non-metric traits were observable within this grouping

5. The benefits of the four-stage approach to re-association

The landmark-based MNI of nine for the MNS collection (all excavations) was derived from left femoral fragments. This calculation assumed a minimum number of left femora possibly interred in Excavation II (n = 1), even though a left femur was not identifiable from those remains. Fragments included in the MNI represented only a

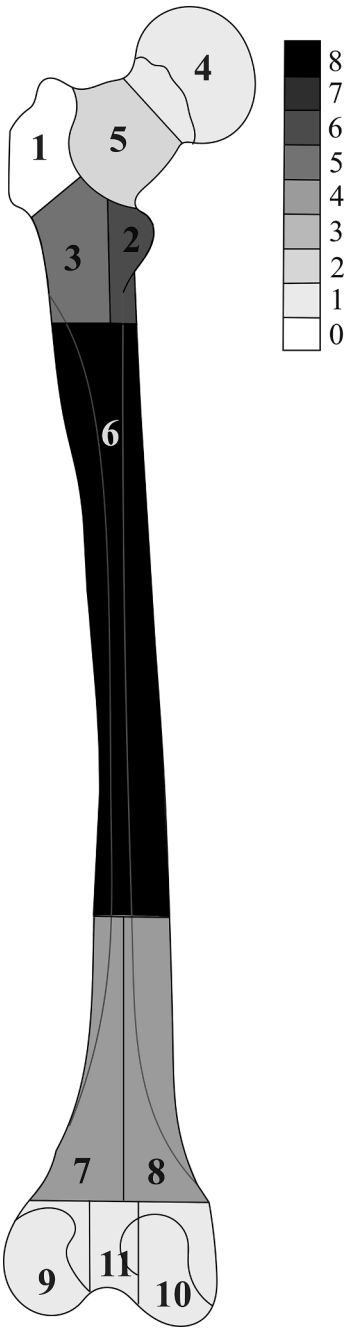

Fig. 5. Zone representation of femoral fragments used in the landmark-based MNI calculation. The scale bar indicates how many of the eight (all femora included in MNI, excluding Excavation II) left femora include the zone indicated on the drawing. Drawing revised from original by Caroline Erolin (née Needham), University of Dundee, in Knüsel and Outram's (2004) *Fragmentation: The Zonation Method Applied to Fragmented Human Remains from Archaeological and Forensic Contexts* (Figure 9).

focused portion of the femur, namely the diaphyseal region, or zone 6 (Fig. 5). Thus, there was very little representation of articular facets or major entheses.

If individuals within the MNS population were represented solely by the MNI, little information about life-history would be ascertainable because an Individual would have been represented by only one fragment. As noted by Anderson (1964, as cited by Glencross, 2014), this would have limited any analysis to a specific element (or portion of element) rather than allowing for the examination of multiple bones whose condition as a group would provide more detailed information on

life-history. This was illustrated by the femora comprising the MNI, which represented a specific area of the bone, namely the diaphysis. As such, the MNI was most useful in this study as an indication of the minimum population size, upon which to reference our other findings, but not as a representation of individuals. The re-association of groups of elements and fragments into Individuals or Associations allowed for increased skeletal representation and higher quality data, which in turn facilitates more detailed future research with higher analytical potential.

By using a four-stage approach to re-associate the fragmented and commingled remains from MNS, groupings of multiple bones were compiled to represent discrete Individuals or groupings of fragments from the same individual whose relationship with other groupings could not be ruled out (Associations). Referring to the process of elimination between our identified Individual and Association groupings (Table 4), at least seven discrete people were represented. In addition to the five discrete Individuals identified within this study, the Associations account for at least two more distinct people. When compared to Pezhemsky's groupings (Bazaliiskii et al., 2016), our results indicated clear differences. Pezhemsky's were more numerous and spatially distributed, with higher spatial variation, than those found in this study (Fig. 6).

Compared to the MNI, our multi-method approach accounted for fewer Individuals, but was able to provide more information on life-history. This was especially true in comparison to Pezhemsky's MNI estimate, which provided little information on individuals. As Pezhemsky's estimate was not based on any reported methods, we are unable to ascertain the accuracy of his approach compared to ours. In fact, neither of these methods can be tested for accuracy because of the unknown size and composition of MNS. This contextual constraint is inherent to most archaeological human remains, especially those that are fragmented and commingled, such as through unintentional destructive processes. However, we are confident in the transparency and replicability of our methodology. The four-stage approach presented here was more useful for the study of individual life-history and provided a more meaningful account of the human remains from MNS.

6. Conclusions

This study identified five discrete Individuals from 1245 human bone fragments. Eight other Associations (groupings that may or may not be associated with one another or the Individual groupings) were also identified. From these we were able to determine that these Individual/Association groupings collectively represented at least seven people. This was compared to the independent landmark-based MNI of nine individuals based on femoral diaphyseal fragments. Of the 1245 fragments in the MNS collection, 16.23% were able to be refit into 74 conjoins. This collection included one likely juvenile individual; all other fragments appeared to be from adults. These findings were inconsistent with Dr. Pezhemsky's original estimate of 19 adult individuals (Bazaliiskii et al., 2016).

The application of multiple methods under a staged process to re-associate human remains from highly fragmented and commingled collections into discrete individuals allowed for a more detailed study of an individual, including their non-metric traits, entheseal morphology, and pathological changes. Through individualization, we were able to better describe the individual life histories of those interred at this site. By applying a set of clearly outlined methods, we were able to make more comprehensive groupings supported by a wide range of evidence. The use of zooarchaeological, bioarchaeological, and forensic anthropological methods will allow other scholars to emulate, challenge, or

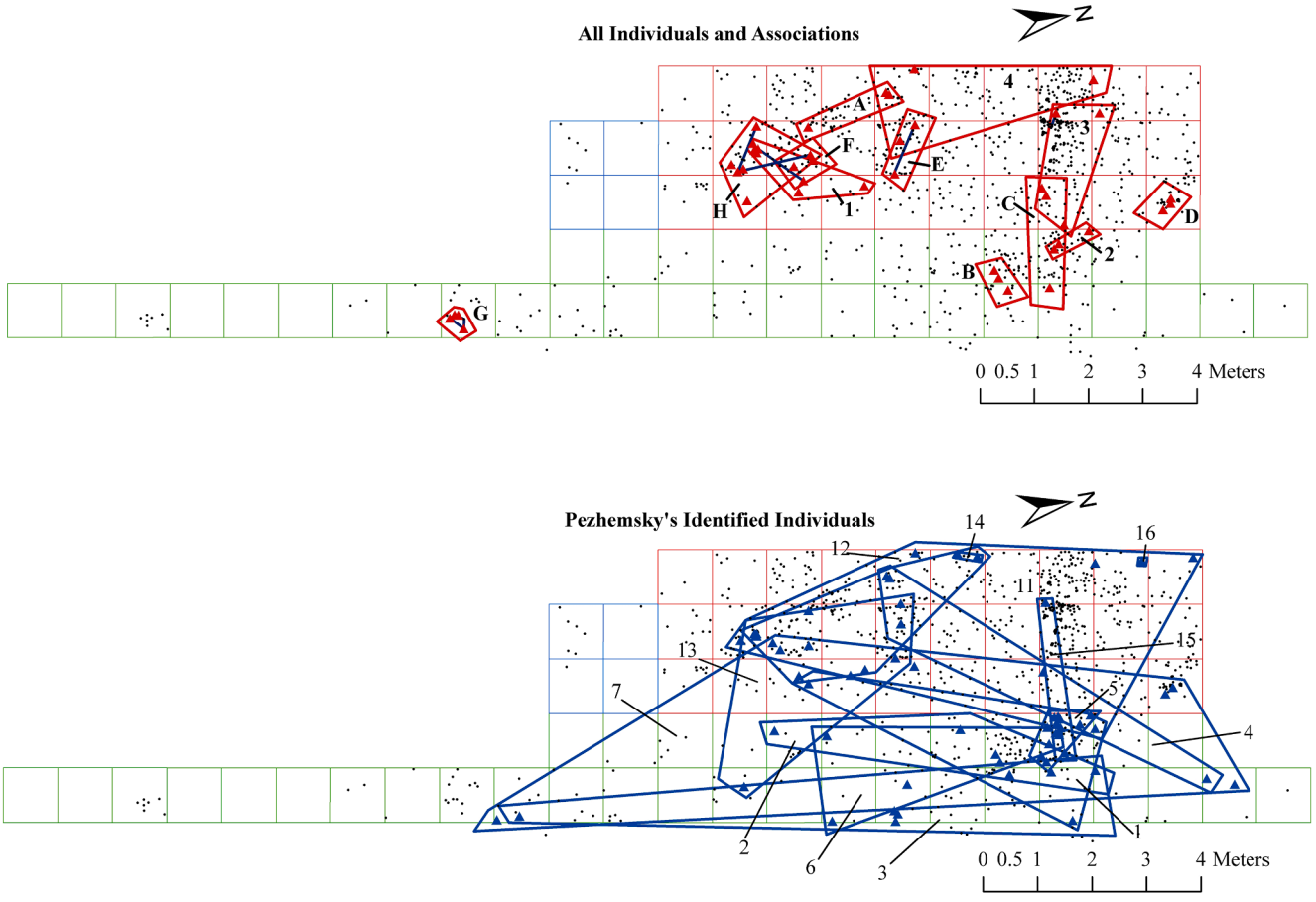

Fig. 6. Comparison of the spatial distribution of MNS groupings using our four-stage approach (top) and Pezhemsky's identified individuals (bottom).

add to our findings in the future. This approach would greatly benefit from being tested on an experimental collection or known population in order to examine its efficacy. Further, DNA analysis would also help to evaluate the accuracy of the groupings made in this study. Nonetheless, the four-stage nature of this method makes it applicable to a wide range of contexts that vary in preservation and depositional history. Considering the high level of fragmentation of the MNS collection, this includes even the lower ends of the preservation spectrum. Continuing to study skeletal collections beyond their MNI values allows for more detailed bioarchaeological analysis and sets the scene for future research. Re-associating fragmented and commingled human remains into discrete individuals is important in contexts where cemeteries (most frequently unmarked cemeteries) are destroyed during the development of land or through erosion, including other disruptions associated with climate change. Projects to salvage information from damaged remains are more meaningful if they are able to restore a sense of individuality for the sake of reburial or the return of remains to descendants.

Declaration of Competing Interest

The authors declare that they have no known competing financial interests or personal relationships that could have appeared to influence the work reported in this paper.

Acknowledgements

This research was conducted as a part of the Baikal Archaeology Project (BAP), directed by Andrzej W. Weber, University of Alberta (https://baikalproject.artsrn.ualberta.ca/) and largely funded by the Social Sciences and Humanities Research Council of Canada Partnership Grant [grant no. 895-2018-1004]. Funding was also provided by the Northern Scientific Training Program (Polar Knowledge) and the University of Saskatchewan. We would also like to thank William T.D. Wadsworth (University of Alberta) for GIS help, as well as committee member Dr. Ernest Walker (University of Saskatchewan) and external examiner Dr. Lesley Harrington (University of Alberta). Due to a discontinuous culture-history in this area, both genetically and based on oral history, consultation with populations directly descendent of the people whose remains are included in this study was not possible. Ethics approval was obtained from the research ethics boards of both the University of Saskatchewan [BIO–1881], where this research took place, and the University of Alberta [00089535], where the BAP project is based.

References:

Acsádi, G., Nemeskéri, J., 1970. History of the Human Life Span and Mortality. Akadémiai Kiadó, Budapest.

Adams, B.J., Byrd, J.E., 2006. Resolution of small-scale commingling: a case report from the Vietnam War. Forensic Sci. Int. 156, 63–69. https://doi.org/10.1016/j.forsciint.2004.04.088.

Adams, B.J., Konigsberg, L.W., 2008. How Many People? Determining the number of individuals represented by commingled human remains. In: Adams, B.J., Byrd, J.E. (Eds.), Recovery, Analysis, and Identification of Commingled Human Remains. Humana Press, Totowa, NJ, pp. 241–255. https://doi.org/10.1007/978-1-59745-316-5_12.

Anderson, J.E., 1964. The people of Fairty: an osteological analysis of an Iroquois ossuary. National Museum Canada Bull. 193, 28–129.

Auerbach, B.M., Ruff, C.B., 2010. Stature Estimation Formulae for Indigenous North American Populations. Am. J. Phys. Anthropol. 141, 190–207. https://doi.org/10.1002/ajpa.21131.

Bass, W.M., 1995. Human Osteology: A Laboratory Field Manual. Missouri Archaeological Society, Columbia, SC.

Bazaliiskii, V.I., Peskov, S.A., Shchetnikov, A.A., Tyutrin, A.A., 2016. Early-Neolithic cemetery of Moty-Novaya Shamanka in the valley of the Irkut River [In Russian]. Irkutsk State Univ. Geoarchaeol. Ethnogr. Anthropol. Ser. 18, 40–72.

Behrensmeyer, A.K., 1978. Taphonomic and ecologic information from bone weathering. Paleobiology 4 (2), 150–162. https://doi.org/10.1017/S0094837300005820.

Bourgeois, R.L., 2020. A Multi-Method Approach to Re-Associating Fragmented and Commingled Human Remains (Master's thesis, University of Saskatchewan, Saskatoon, Canada). Retrieved from https://harvest.usask.ca/handle/10388/13041. 2020.

Bronk Ramsey, C., Schulting, R.J., Bazaliiskii, V.I., Goriunova, O.I., Weber, A.J., 2021. Spatio-temporal patterns of cemetery use among Middle Holocene hunter-gatherers of Cis- Baikal, Eastern Siberia. Archaeol. Res. Asia 25, 100253.

Brothwell, D.R., 1981. Digging Up Bones. Cornell University Press, Ithaca, NY.

Buikstra, J.E., Ubelaker, D.H., 1994. Standards for Data Collection from Human Skeletal Remains. Arkansas Archaeological Survey Research Series No, Arkansas, p. 44.

Byrd, J.E., 2008. Models and methods for osteometric sorting. In: Adams, B.J., Byrd, J.E. (Eds.), Recovery, Analysis, and Identification of Commingled Human Remains. Humana Press, Totowa, NJ, pp. 199–220. https://doi.org/10.1007/978-1-59745-316-5_10.

Byrd, J.E., Adams, B.J., 2003. Osteometric sorting of commingled human remains. J. Forensic Sci. 48 (4), 717–724.

Byrd, J.E., LeGarde, C.B., 2014. Osteometric sorting. In: Adams, B.J., Byrd, J.E. (Eds.), Commingled Human Remains: Methods in Recovery, Analysis, and Identification. Elsevier Science & Technology, New York, NY, pp. 167–192.

De Mendonça, M.C., 2000. Estimation of height from the length of long bones in a Portuguese adult population. Am. J. Phys. Anthropol. 112, 39–48. https://doi.org/10.1002/(SICI)1096-8644(200005)112:1<39::AID-AJPA5>3.0.CO;2-%23.

Dobney, K., Reilly, K., 1988. A method for recording archaeological animal bones: the use of diagnostic zone. Circaea 5 (2), 79–96.

Finlayson, J.E., Bartelink, E.J., Perrone, A., Dalton, K., 2017. Multimethod resolution of a small-scale case of commingling. J. Forensic Sci. 61 (2), 493–497. https://doi.org/10.1111/1556-4029.13265.

Finnegan, M., 1978. Non-metric variation of the infracranial skeleton. J. Anat. 125, 23–37.

Foster, G.A., Lovekamp, W.E., 2015. Disasters and cemeteries: a clarion call for matters of grave urgency. AGS Quart. 39 (3), 14–19.

Gestsdóttir, H., 2014. Osteoarthritis in In Iceland: An archaeological study (Doctoral Dissertation, University of Iceland, Reykjavík, Iceland). Retrieved from. https://skemman.is/bitstream/1946/20512/1/Dr.%20Hildur%20Gestsd%C3%B3ttir.pdf.

Glencross, B., 2014. Into the Kettle: the analysis of commingled remains from Southern Ontario. In: Osterholtz, A.J., Baustian, K.M., Martin, D.L. (Eds.), Commingled and disarticulated human remains: Working toward improved theory, method, and data. Springer, New York, NY, pp. 67–82. https://doi.org/10.1007/978-1-4614-7560-6_5.

Hauser, G., De Stefano, G.F., 1989. Variations in the form of the hypoglossal canal. Am. J. Phys. Anthropol. 67, 7–11.

Herrmann, N.P., Devlin, J.B., 2008. Assessment of commingled human remains using a GIS-based approach. In: Adams, B.J., Byrd, J.E. (Eds.), Recovery, Analysis, and Identification of Commingled Human Remains. Humana Press, Totowa, NJ, pp. 257–269. https://doi.org/10.1007/978-1-59745-316-5_13.

Karell, M.A., Langstaff, H.K., Halazonetis, D.J., Minghetti, C., Frelat, M., Kranioti, E.F., 2016. A novel method for pair-matching using three-dimensional digital models of bone: mesh-to-mesh value comparison. Int. J. Legal Med. 130, 1315–1322. https://doi.org/10.1007/s00414-016-1334-3.

Killoran, P., Pollack, D., Nealis, S., Rinker, E., 2016. Cemetery preservation and beautification of death: investigations of unmarked early to mid-nineteenth-century burial grounds in Central Kentucky. In: Osterholtz, A.J. (Ed.), Theoretical Approaches to Analysis and Interpretation of Commingled Human Remains. Springer, New York, NY, pp. 219–241. https://doi.org/10.1007/978-3-319-22554-8_11.

Knüsel, C.J., Outram, A.K., 2004. Fragmentation: the zonation method applied to fragmented human remains from archaeological and forensic contexts. Environ. Archaeol. 9, 85–97. https://doi.org/10.1179/env.2004.9.1.85.

LeGarde, C.B., 2019. Preliminary findings from a visual pair-matching study in a large commingled assemblage. Forensic Anthropol. 2 (2), 65–71. https://doi.org/10.5744/fa.2019.1001.

Lewis, M., 2018. Paleopathology of Children: Identification of Pathological Conditions in the Human Remains of Non-Adults. Academic Press, London, UK.

Lieverse, A.R., Bazaliiskii, V.I., Goriunova, O.I., Weber, A.W., 2009. Upper Limb Musculos keletal stress markers among middle Holocene foragers of Siberia's Cis-Baikal Region. Am. J. Phys. Anthropol. 138, 458–472. https://doi.org/10.1002/ajpa.20964.

Lieverse, A.R., Mack, B., Bazaliiskii, V.I., Weber, A.W., 2016. Revisiting osteoarthritis in the Cis-Baikal: understanding behavioural variability and adaptation among middle Holocene foragers. Quat. Int. 405, 160–171. https://doi.org/10.1016/j.quaint.2015.03.019.

Lieverse, A.R., Metcalf, M.A., Bazaliiskii, V.I., Weber, A.W., 2008. Pronounced bilateral asymmetry of the complete upper extremity: a case from the early neolithic Baikal, Siberia. Int. J. Osteoarchaeol. 18, 219–239. https://doi.org/10.1002/oa.935.

Lieverse, A.R., Weber, A.W., Bazaliiskiy, V.I., Goriunova, O.I., Savel'ev, N.A., 2007. Osteoarthritis in Siberia's Cis-Baikal: skeletal indicators of hunter-gatherer adaptation and cultural change. Am. J. Phys. Anthropol. 132, 1–16. https://doi.org/10.1002/ajpa.20479.

Mack, J.E., Waterman, A.J., Racila, A.-M., Artz, J.A., Lillios, K.T., 2016. Applying zooarchaeological methods to interpret mortuary behaviour and taphonomy in commingled burials: the case study of the late neolithic site of Bolores, Portugal. Int. J. Osteoarchaeol. 26, 524–536. https://doi.org/10.1002/oa.2443.

Maples, J.N., East, E.A., 2013. Destroying mountains, destroying cemeteries: historic mountain cemeteries in the coalfields of boone, Kanawha, and Raleigh Counties, West Virginia. J. Appalachian Stud. 19 (1/2), 7–26.

Mays, S., Holst, M., 2006. Palaeo-otology of Cholesteatoma. Int. J. Osteoarchaeol. 16, 1–15. https://doi.org/10.1002/oa.801.

Mead, S.B., Christensen, A.M., 2020. Bilateral asymmetry of nutrient foramen position in the human femur and tibia. Forensic Anthropol. 3 (1), 36–38.

Moore-Jansen, P.H., Jantz, R.L., Ousley, Stephen D., 1994. Data Collection Procedures for Forensic Skeletal Material. Forensic Anthropology Center, Dept. of Anthropology, University of Tennessee, Knoxville, TN.

Mundorff, A.Z., Shaler, R., Bieschke, E., Mar-Cash, E., 2014. Marrying anthropology an DNA: essential for solving complex commingling problems in cases of extreme fragmentation. In: Adams, B., Byrd, J. (Eds.), Recovery, Analysis, and Identification of Commingled Human Remains. Humana Press, Totowa, NJ, pp. 285–299. https://doi.org/10.1016/B978-0-12-405889-7.00012-5.

Oettlé, A.C., Demeter, F.P., L'Abbé, E.N., 2017. Ancestral Variation in the Shape and Size of the Zygoma. The Anatomical Record 300, 196–208. https://doi.org/10.1002/ar.23469.

Ortner, D.J., 2003. Osteoarthritis and Diffuse Idiopathic Skeletal Hyperostosis. In: Identification of Pathological Conditions in Human Skeletal Remains. Academic Press, San Diego, CA, pp. 545–560.

Osterholtz, A.J., 2012a. The social role of hobbling and torture: violence in the prehistoric Southwest. Int. J. Paleopathol. 2, 148–155. https://doi.org/10.1016/j.ijpp.2012.09.011.

Osterholtz, A.J., 2012b. The social role of hobbling and torture as performative violence: an example from the Prehistoric Southwest. Kiva: J. Southwestern Anthropol. History 78 (2), 123–144. https://doi.org/10.1179/kiv.2012.78.2.002.

Osterholtz, A.J., 2014. Extreme processing at mancos and sacred ridge: the value of comparative studies. In: Osterholtz, A.J., Baustian, K.M., Martin, D.L. (Eds.), Commingled and Disarticulated Human Remains: Working Toward Improved Theory, Method, and Data. New York, NY, Springer, pp. 105–127. https://doi.org/10.1007/978- 1-4614-7560-6_7.

Osterholtz, A.J., 2018. Interpreting and reinterpreting sacred ridge: placing extreme processing in a larger context. Kiva: J. Southwestern Anthropol. History 84 (4), 461–479. https://doi.org/10.1080/00231940.2018.1533197.

Osterholtz, A.J., Baustian, K.M., Martin, D.L., 2014a. Introduction. In: Osterholtz, A.J., Baustian, K.M., Martin, D.L. (Eds.), Commingled and Disarticulated Human Remains: Working Toward Improved Theory, Method, and Data. New York, NY, Springer, pp. 1–13. https://doi-org /10.1007/978-1-4614-7560-6_1.

Osterholtz, A.J., Baustian, K.M., Martin, D.L., Potts, D.T., 2014b. Commingled human skeletal assemblages: integrative techniques in determination of the MNI-MNE. In: Osterholtz, A.J., Baustian, K.M., Martin, D.L. (Eds.), Commingled and Disarticulated Human Remains: Working Toward Improved Theory, Method, and Data. Springer, New York, NY, pp. 35–50. https://doi.org/10.1007/978-1-46ss14-7560-6_3.

Outram, A.K., Knüsel, C.J., Knight, S., Harding, A.F., 2005. Understanding complex fragmented assemblages of human and animal remains: a fully integrative approach. J. Archaeol. Sci. 32, 1699–1710. https://doi.org/10.1016/j.jas.2005.05.008.

Outram, A.K., 1998. The Identification of Palaeoeconomic Context of Prehistoric Bone Marrow and Grease Exploitation (Doctoral dissertation, Durham University, Durham, England). Retrieved from http://etheses.dur.ac.uk/1432/.

Outram, A.K., 2001. A new approach to identifying bone marrow and grease exploitation: why the "indeterminate" fragments should not be ignored. J. Archaeol. Sci. 28, 401–410. https://doi.org/10.1006/jasc.2000.0619.

Perrone, A., Finlayson, J.E., Bartelink, E.J., Dalton, K.D., 2014. Application of portable X-ray fluorescence (XRF) for sorting commingled human remains. In B.J. Adams, J.E. Byrd (Eds.) Commingled Human Remains: Methods in Recovery, Analysis, and Identification. Oxford, UK: Academic Press, pp. 145–166. https://doi.org/10.1016/B978- 0-12-405889-7.00007-1.

Purchase, S.L., 2016. Infectious Disease as an Indicator of Physiological Stress in the Middle Holocene Cis-Baikal (Master's thesis). Retrieved from https://harv est.usask.ca/bitstream/handle/10388/7512/PURCHASE-THESIS- 2016.pdf?sequence=1&isAllowed=y.

Rainville, L., 2009. Protecting our shared heritage in African-American Cemeteries. J. Field Archaeol. 34 (2), 196–206. https://doi.org/10.1179/009346909791071005.

Reddi, A.H., 1981. Cell biology and biochemistry of endochondral bones development. Collagen Related Res. 1 (2), 209–226. https://doi.org/10.1016/S0174- 173X(81)80021-0.

Rodrìguez, J.M.G., Hackman, L., Martínez, W., Medina, C.S., 2016. Osteometric sorting of skeletal elements from a sample of modern Colombians: a pilot study. Int. J. Legal Med. 30, 541–550. https://doi.org/10.1007/s00414-015-1142-1.

Saunders, S., 1978. The Development and Distribution of Discontinuous Morphological Variation of the Human Infracranial Skeleton. *Musée National de l'Homme. Collection Mercure. Commission Archéologique du Canada*. Publications d'Archéologie. Dossier Ottawa 81, 1–534.

Schaefer, M., Black, S., Scheuer, L., 2009. Juvenile Osteology, a Laboratory and Field Manual. Academic Press, New York, NY.

Scott, E.C., 1979. Dental wear scoring technique. Am. J. Phys. Anthropol. 51, 213–218. https://doi.org/10.1002/ajpa.1330510208.

Smith, B.H., 1984. Patterns of molar wear in hunter-gatherers and agriculturalists. Am. J. Phys. Anthropol. 63, 39–56. https://doi.org/10.1002/ajpa.1330630107.

Steele, D.G., 1970. Estimation of stature from fragments of long limb bones. Personal identification in mass disasters, 85.

Steele, D.G., McKern, T.W., 1969. A method for assessment of maximum long bone length and living stature from fragmentary long bones. Am. J. Phys. Anthropol. 31, 215–227. https://doi.org/10.1002/ajpa.1330310211.

Stock, J.T., Bazaliiskii, V., Goriunova, O.I., Savel'ev, N.A., Weber, A.W., 2010. Skeletal morphology, climatic adaptation, and habitual behavior among mid-holocene cis-baikal populations. In: Weber, A.J., Katzenberg, M.A., Schurr, T.G. (Eds.), Prehistoric Hunter-Gatherers of the Baikal Region, Siberia: Bioarchaeological Studies of Past Life Ways. University of Pennsylvania Museum of Archaeology and Anthropology, Pennsylvania, pp. 193–216.

Suwa, G., 1990. A comparative analysis of hominid dental remains from the Shungura and Usno formation, Omo Valley, Ethiopia (Unpublished doctoral thesis). University of California Berkeley, Berkeley, USA.

Temple, D.H., Bazaliiskii, V.I., Goriunova, O.I., Weber, A.W., 2014. Skeletal growth in early and late neolithic foragers from the cis-baikal region of Eastern Siberia. Am. J. Phys. Anthropol. 153, 377–386. https://doi.org/10.1002/ajpa.22436.

Thomas, R.M., Ubelaker, D.H., Byrd, J.E., 2013. Tables for the metric evaluation of pair-matching of human skeletal elements. J. Forensic Sci. 58 (4), 952–956. https://doi.org/10.1111/1556-4029.12133.

Ubelaker, D.H., 2002. Approaches to the study of commingling in human skeletal biology. In: Haglund, W.D., Sorg, M.H. (Eds.), Advances in Forensic Taphonomy: Method, Theory, and Archaeological Perspectives. CRC Press, Florida.

United Nations Educational, Scientific and Cultural Organization, 2018. World Heritage in Danger. Electronic document, https://whc.unesco.org/en/158, accessed October 20, 2018.

Vehit, U., Christensen, A.M., 2019. Bilateral asymmetry of nutrient foramen position in forearm bones: implications for its use in sorting commingled remains. J. Forensic Sci. 64, 186–189. https://doi.org/10.1111/1556-4029.13853.

Weber, A.W., McKenzie, H.G., Beukens, R., 2010. Radiocarbon Dating of Middle Holocene Culture History in Cis-Baikal. In: Weber, A.W., Katzenberg, M.A., Schurr, T.G. (Eds.), Prehistoric Hunter-Gatherers of the Baikal Region, Siberia: Bioarchaeological Studies of Past Life Ways. University of Pennsylvania Museum of Archaeology and Anthropology, Pennsylvania, pp. 30–49.

Weber, A.W., Bronk Ramsey, C., Schulting, R.J., Bazaliiskii, V.I., Goriunova, O.I., 2021. Midd le Holocene hunter-gatherers of Cis-Baikal, Eastern Siberia: chronology and dietary trends. Archaeol. Res. Asia 25, 100234.

White, T.D., Black, M.T., Folkens, P.A., 2012. Human Osteology. Academic Press, Burlington.

White, T.D., 1977. New Fossil hominids from Laetolil, Tanzania. Am. J. Phys. Anthropol. 46, 197–230. https://doi.org/10.1002/ajpa.1330460203.

Winder, S.S., 1981. Infracranial Nonmetric Variation: An Assessment of its Value for Biological Distance Analysis (Unpublished doctoral dissertation). Indiana University, Ann Arbor, USA.

Wright, L.E., Vásquez, M.A., 2003. Estimating the length of incomplete long bones: forensic standards from Guatemala. Am. J. Phys. Anthropol. 120, 233–251. https://doi.org/10.1002/ajpa.10119.

Zejdlik, K.J., 2014. Unmingling commingled museum collections: a photographic method. In: Osterholtz, A.J., Baustian, K.M., Martin, D.L. (Eds.), Commingled and Disarticulated Human Remains: Working Toward Improved Theory, Method, and Data. Springer, New York, NY, pp. 173–192. https://doi.org/10.1007/978-1-4614-7560-6_10.